

Microscopic molecular translational dynamics in cholesteric and cholesteric blue phases

Makina Saito, et al. [full author details at the end of the article]

Published online: 05 December 2019
© Springer Nature Switzerland AG 2019

Abstract

In the nematic (*N*) phase, the molecular symmetry axis orients on average along one direction denoted as the director. The cholesteric (*Ch*) phase shows similar orientational order locally. However, the average molecular direction in the *Ch* phase rotates continuously around a direction perpendicular to the director. The cholesteric blue phase (*ChBP*) shows a double-twist orientational order that differs from the single-twist order of the *Ch* phase and also shows self-assembled three-dimensional lattice structure of defect lines of the orientational order in the mesoscopic spatial scale. The helical structure of the molecular orientation in *ChBP* brings the structural colour and photonic band gap into the wavelength range of visible light. Therefore, *ChBP* has been studied for applications to photonic elements and fast-response displays. We measured the molecular translational dynamics along the molecular long axis in the *Ch* phase, *ChBP* and the isotropic (*Iso*) liquid phase of the mixture system of the nematic liquid crystal 4'-heptyloxy-4-biphenylcarbonitrile and the chiral dopant (S)-4'-(2-methylbutyl)-4-biphenylcarbonitrile directly at the nanometric molecular scale by using quasi-elastic scattering spectroscopy using Mössbauer gamma ray. We successfully determined the timescale of the molecular translational motion in the *Ch* phase to be 40 ns, which is similar to the timescale of the *N* phase of 4'-n-octyl-4-cyanobiphenyl. In the *ChBP* and *Iso* phase, molecular motions occur on timescales similar to those of the *Ch* phase, suggesting that the molecular dynamics is insensitive to the presence of orientational order, the helical structure, and higher-order structure. Our results demonstrate that the molecular dynamics in both the *Ch* phase and *ChBP* can be measured by quasi-elastic gamma-ray-scattering spectroscopy, in addition to the time scales of molecular motions in the *N* and smectic phases. The present results greatly expand the possibility of using this spectroscopic technique for molecular-mobility studies of industrial liquid-crystalline materials, because *Ch* liquid crystals are widely used for display systems in addition to *N* liquid crystals.

Keywords Liquid crystal · Cholesteric phase · Cholesteric blue phase · Quasi-elastic scattering · Time-domain interferometry · Mössbauer gamma ray

1 Introduction

Liquid crystal phases are an intermediate state between the liquid and crystalline phases; these exhibit structural anisotropy and related orders, which propagate over much longer spatial ranges than the microscopic scale order seen in liquids [1, 2]. Various liquid crystal phases showing a variety of orders have been found to date [1, 2]. In the nematic (*N*) phase, widely used for twisted nematic-display systems, the symmetry axis of molecules orients on average along one dimension denoted as the *director*. For rod-like molecules, the long axis of the molecules is oriented along the director. In the cholesteric (*Ch*) phase, rod-like molecules show local orientational order, as in the *N* phase; however, the average molecular direction rotates continuously around a direction perpendicular to the director. This rotational property of the *Ch* phase usually originates from the chirality of the molecules. In the *Ch* phase, the molecules form a helical structure of molecular directions with a well-defined spatial period. In one direction, the *Ch* phase therefore shows optical activity, circular dichroism and wavelength selectivity of transmission/reflection—which produces a photonic bandgap and structural colour—in the visible-light regime. The pitch of the helical structure in the *Ch* phase can be changed either by an external field or by temperature, owing to the soft response of the *Ch* phase that originates from its internal molecular mobility. Capitalising on these unique properties, the *Ch* phase is used for liquid-crystal display, thermometers, and ornaments and has been studied for application as a laser medium [3, 4].

The cholesteric blue phase (*ChBP*) is sometimes observed in the temperature range between the *Ch* and isotropic (*Iso*) liquid phases. The microscopic structure of this phase has a double-twist orientational order that differs from the single-twist order of the *Ch* phase [5, 6]. The free energy of the double-twist molecular order is microscopically lower than that of the single-twist order, because the former more closely satisfies the requirement of molecular chirality. However, the double-twist order cannot fill three-dimensional space, and defect regions always arise. *ChBP* is stabilised by spontaneously creating a three-dimensional lattice structure of defect lines to minimise the entire free energy [7, 8]. *ChBPs* are classified into the three phases *ChBP*_I–*ChBP*_{III} according to the symmetry of the three-dimensional lattice structure: simple cubic, body-centred cubic, or amorphous, respectively [7–11]. Because the lattice periods of *ChBP* are often several hundred nm, *ChBP* exhibits an isotropic three-dimensional photonic bandgap and structural colour in the range of visible light. Moreover, its response time for electro-optical switching has been found to be much shorter than for other typical liquid-crystal phases [12]. Therefore, *ChBP* has been widely studied for the development of unique photonic elements [13] and fast-response displays [12]. However, *ChBP* is stable only in a very limited temperature range, typically a few Kelvins. This property makes its application very challenging. To overcome this difficulty, polymer-stabilisation of *ChBP* has been attempted, and it has been found that *ChBP* can be stabilised over a much wider temperature range, such as 60 K and including room temperature [12, 14].

Molecular mobility plays an important role in the fast response of the director to an electric field. However, microscopic pictures of the molecular translational dynamics in the *Ch* phase and *ChBP* are not well-established. Recently, the molecular translational dynamics of the *N* and smectic (*Sm*) phases along the direction of the molecular long axis have been studied by

quasi-elastic Mössbauer gamma-ray-scattering (QEGS) spectroscopy. These investigations employed time-domain interferometry using the ^{57}Fe nuclear resonance, which has a 4.7-neV energy resolution [15–17]. These studies revealed that QEGS has enough spatial and energy resolution to resolve the molecular translational motions along the molecular long axis in the *N* and *Sm* phases of typical liquid crystal systems [18, 19]. Because the molecular orientational order in the *Ch* phase and *ChBP* is similar to that of the *N* phase on the microscopic scale, the time scale of molecular motions in the *Ch* phase and *ChBP* is expected to be similar to that of the *N* phase. Therefore, QEGS is also suitable for studying the molecular dynamics in the *Ch* phase and *ChBP*. The purpose of the present study is to use QEGS to understand how the presence of the orientational order, helical order, and higher-order structures of *ChBP* affect the microscopic molecular dynamics. We thereby demonstrate that QEGS is suitable for the direct study of molecular mobility in industrial liquid-crystalline materials, including *Ch* liquid crystals.

2 Experiment

We focus on systems consisting of mixtures of the nematic liquid crystal 4'-heptyloxy-4-biphenylcarbonitrile (7OCB) and the chiral dopant (S)-4'-(2-methylbutyl)-4-biphenylcarbonitrile (CB15), both purchased from Merck (Darmstadt, Germany). We performed optical microscope observations of the mixture samples, with molar fractions ϕ of CB15 between $\phi=0$ and 0.5. We employed a polarised microscope (BX61, Olympus) with crossed-Nicols polarisers.

We performed X-ray diffraction studies in the region $q=1\text{--}5\text{ nm}^{-1}$ for the mixture sample with $\phi=0.5$, which shows *ChBP*, by using Cu-K α X-rays in a Nanopix (Rigaku, Tokyo, Japan). Here $q=4\pi/\lambda\sin(\theta/2)$ is the magnitude of the momentum transfer (wave-vector transfer), where λ is the wavelength of the incident X-rays, and θ is the scattering angle.

We performed QEGS experiments on the mixture sample with $\phi=0.5$ at the nuclear-resonance scattering beamline (BL09XU) of SPring-8 (Japan) in an operating mode with a bunch interval of 684.3 ns. We used a multiline gamma-ray time-domain interferometry system in the driving-emitter condition for the QEGS experiments. We utilised directional Mössbauer gamma-rays (with an energy of 14.4 keV and an energy width of ~ 4.7 neV) from the ^{57}Fe nucleus for the QEGS measurements [17], and we employed multi-element Si-avalanche photodiode (APD) detectors to detect the scattered gamma rays. We placed the APD detectors at the angle corresponding to the peak of the small-angle scattering, $q \sim 2.5\text{ nm}^{-1}$. The detector covers the q region between 1.5 and 4.4 nm^{-1} , which includes the entire small-angle diffraction peak at all measurement temperatures: 306 K, 308 K and 310 K. In the previous study, the external magnetic field which is too weak to affect the molecular dynamics has been used to align the molecular orientation for the purpose to suppress the layer undulation and increase the scattering intensity [19]. In this experiment, the external magnetic field was not applied for *Ch* phase and *ChBP* because the molecular orientation in the *Ch* phase and *ChBP* cannot be uniformly aligned to one direction. Therefore, the molecules randomly orient to the direction of the incident gamma rays. The APD detector covers the entire azimuthal-angle distribution of the small-angle scattering. We controlled the sample temperature with a heater system, using in-situ observations of the sample to determine the phase.

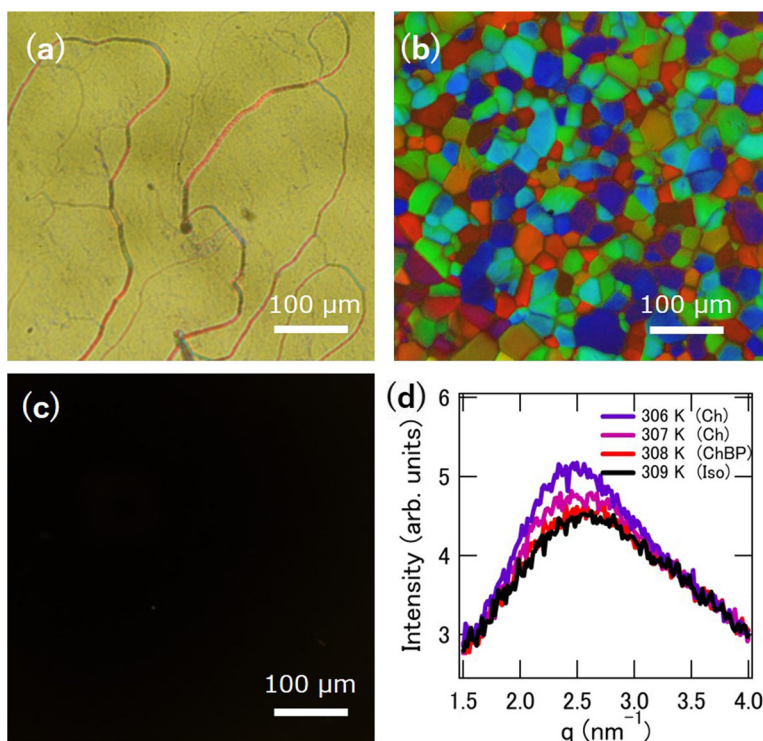


Fig. 1 Microphotographs and small-angle X-ray diffraction spectra. Microphotographs for (a) the *Ch* phase, (b) *ChBP*, and (c) the *Iso* phase. Scale bars equal to 100 μm . (d) Small-angle X-ray-diffraction spectra obtained at the temperatures 306 K, 307 K, 308 K, and 309 K

3 Results and discussion

In Fig. 1, we show examples of microphotographs obtained at (a) 307 K, (b) 308 K and (c) 311 K for the sample with $\phi = 0.5$ under crossed-Nicols polarisers. We observed the unique oily-streak texture of the *Ch* phase and the platelet texture of *ChBP* (*ChBP_H*), as shown in Fig. 1a and b, respectively, and we used them for phase identification. In contrast, the dark image shown in Fig. 1c suggests the *Iso* phase. The phase diagram we obtained is shown in Fig. 2.

The small-angle X-ray diffraction spectra obtained for the sample with $\phi = 0.5$ are shown in Fig. 1d. The peak originates from the spatial correlation of the molecular positions along the molecular long axis. The intensity—which is related to molecular translational order along the molecular long axis—gradually decreases upon heating across the *Ch*-*ChBP* phase-transition temperature and the *ChBP*-*Iso* phase-transition temperature. The peak position, which represents the intermolecular distance along the molecular long axis, changes only slightly. This result suggests that, while the molecular translational order gradually decreases on heating, the local molecular structure is not greatly affected by the temperature change.

In Fig. 3a, we present examples of the QEGS time spectra obtained for the sample with $\phi = 0.5$ at the temperatures 306 K, 308 K and 310 K. We confirmed that the sample is in the *Ch* phase, *ChBP* and *Iso* phase by in-situ observations by naked eyes at each temperature. The time spectra, which contain direct information about the molecular translational motion along the molecular long axis at the inter-molecular scale, do not show large changes with increasing

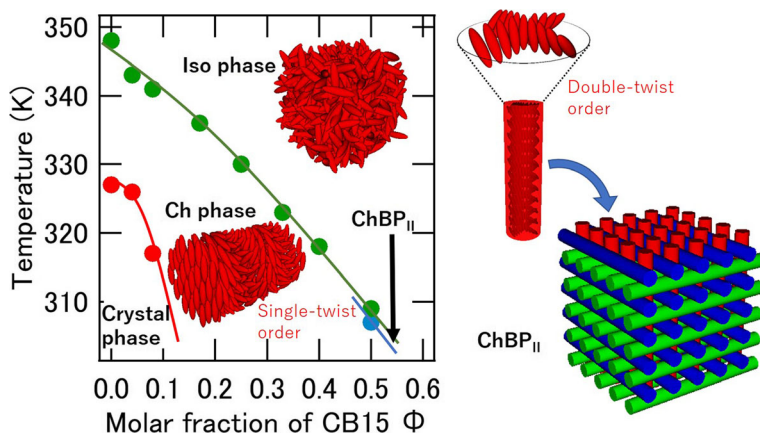


Fig. 2 Phase diagram of the 7OCB-CB15 mixture system. The phase diagram of the 7OCB-CB15 mixture system obtained by optical-microscope observations. We also show images of the molecular arrangements for the *Ch* phase, *ChBP*_{II}, and the *Iso* phase. Here, ϕ indicates the molar fraction of CB15

temperature. This suggests that the timescale of the molecular motion is not greatly affected by the phase transitions. The spectrum shape changes following the normalised intermediate-scattering function, which describes the temporal decay of the spatial correlations of the electron densities with the spatial scale of $\sim 2\pi/q$ in the case of this experiment. The extracted normalised intermediate-scattering functions are shown in Fig. 3b. See Ref. [17] for the details of the data analysis. We performed least-squares fits for the obtained time spectra, assuming an exponential function of the form $f \exp(-t/\tau)$ to describe the relaxation behaviour of the normalised intermediate-scattering function after removal of the effect of the pseudo-relaxation, where t , τ and f represent the time, the relaxation time of the spatial correlations among the positions of adjacent molecules along the molecular long axis, and a factor corresponding to the strength of the relaxation, respectively [18, 19]. f reflects the ratio of photons which is treated to be elastically scattered by the sample in the energy scale of neV and represents the ratio of unrelaxed molecular correlations to those that undergo relaxation processes faster than, typically, nanoseconds [17]. We assume that the relaxation of the microscopic spatial correlations among the molecular positions is mainly induced by the molecular translational motion along the molecular long axis [19]. In this case, τ represents the timescale of this molecular translational motion along the molecular long axis.

The fitting curves we obtained are shown as lines in Fig. 3a. This figure confirms that the fitting can be successfully performed for all spectra. The temperature dependence of τ obtained from these measurements is shown in Fig. 4a. We found that the molecular translational motions along the molecular long axis occur in 40 ns in the *Ch* phase at 306 K, close to the *Ch*-*ChBP* phase-transition temperature in the mixture systems of 7OCB and CB15. This timescale is similar to that of the *N* phase obtained for 4'-n-octyl-4-cyanobiphenyl (8CB), which belongs to the same cyanobiphenyl group as 7OCB [19]. This similarity in the timescale of molecular motions between the *N* and *Ch* phases is explained by the fact that the microscopic structure of *Ch* is similar to that of the *N* phase.

In *ChBP* and in the *Iso* phase at a temperature close to the *ChBP*-*Iso* phase transition, the relaxation occurs in a similar timescale to the case of *Ch*. The f parameters obtained from these studies are shown in Fig. 4b. The value of the f parameter decreases only slightly upon heating,

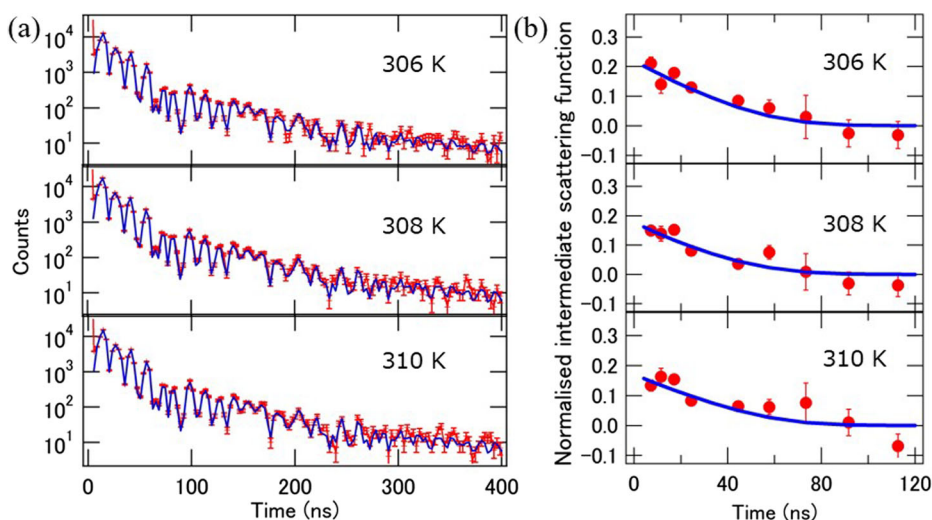


Fig. 3 QEGS Time spectra and extracted intermediate scattering function. **a** Time spectra obtained for the 70CB-CB15 mixture system with $\phi = 0.5$ by QEGS measurements at 306 K, 308 K, and 310 K. The red crosses represent the experimental points and the solid lines are curves obtained by least-squares fitting. **b** Extracted intermediate scattering functions and these exponential relaxation functions obtained by fitting the time spectra

also suggesting the similarity of the dynamics among the samples in the measured temperature range.

Dielectric-relaxation spectroscopy is widely used to study the microscopic molecular rotational dynamics in liquid crystals. For the *Ch* phase of CB15, the relaxation time of the molecular rotational motion around the molecular short axis was previously measured by dielectric-relaxation spectroscopy [20]. This study suggested that the rotational relaxation time in the *Ch* phase is similar to that in the *Iso* phase [20]. For a *ChBP*_{III} system consisting of T-shaped molecules, the relaxation time of the molecular rotational motion around the molecular short axis was also measured by dielectric-relaxation spectroscopy [21]. The characteristic relaxation time in *ChBP*_{III} basically follows the behaviour extrapolated from the behaviour in the *Iso* phase [21]. Thus, the microscopic translational and rotational dynamics are insensitive to the presence of both microscopic orientational order and the mesoscopic structure of *ChBP*.

We therefore conclude that the timescale of the molecular translational motion is at most weakly related to the presence of the higher-order cubic structure, microscopic orientational order and the helical structure. This indicates that we can directly study factors that determine molecular mobility and which are not affected by the orientational order. In contrast, for the *Sm* phase the molecular dynamics are sensitive to the layer order parameter [19]. The present technique is therefore useful for understanding, e.g. surface anchoring effect in the molecular dynamics of the *N* and *Ch* phases.

ChBP is a frustrated phase, because it is stabilised by the frustration between microscopic orientational order and double-twist order. The twist-grain-boundary phase and smectic blue phase (*SmBP*) are other famous frustrated phases, in which the microscopic smectic layered order coexists with the twist order of the molecular orientation [22–24]. In *SmBP*, a high-order mesoscopic lattice structure of defects arises spontaneously [24]. The microscopic layer order is thought to be deformed by the formation of the mesoscopic lattice structure. Because the molecular dynamics is sensitive to the layer order parameter, which is reduced by layer deformation [19], we expect the molecular dynamics to be strongly correlated with the

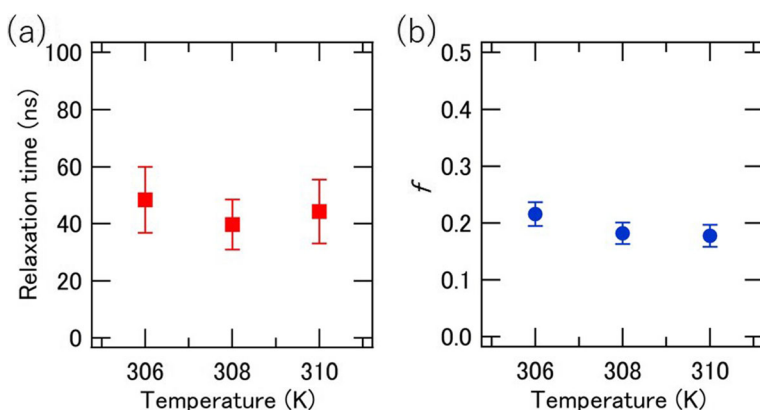


Fig. 4 Experimental values of the relaxation time and the f parameter. **a** The relaxation times and **(b)** the f parameters obtained for the 7OCB-CB15 mixture system with $\phi = 0.5$ by analysing the QEGS time spectra at temperatures 306 K, 308 K, and 310 K. The vertical bars indicate the standard deviations of the statistical errors

formation of the high-order structure of *SmBP*, contrary to the *ChBP* case. Further work on *SmBP* will enable us to understand the general role of the local molecular structure and dynamics on higher-order structures.

4 Conclusions

We have measured the molecular dynamics in the *Ch* phase, *ChBP* and the *Iso* phase of the mixture system of 7OCB and CB15 by using quasi-elastic gamma-ray-scattering spectroscopy. We successfully determined the microscopic timescale of the molecular translational motions in the *Ch* phase along the molecular long axis to be 40 ns, which is similar to the timescale for the *N* phase of 8CB revealed so far. In the *ChBP* and *Iso* phases, the timescale of the molecular translational motion exhibits values similar to the *Ch* case, suggesting that the molecular dynamics along the molecular long axis is insensitive to the presence of orientational order, the helical structure and the higher-order structure. This result is nicely explained by the microscopic molecular-structure picture obtained from our X-ray diffraction studies. Our result demonstrates that the timescale of molecular motions in the *Ch* phase can be determined by quasi-elastic gamma-ray-scattering spectroscopy, in addition to the time scales of molecular motions in the *N* and *Sm* phases. Liquid crystals in the *N* and *Ch* phases are widely used for liquid-crystal displays, e.g., twist nematic-type displays. The present study therefore expands greatly the practicality of this spectroscopic technique to molecular-mobility studies of industrial materials, such as revealing the anchoring effect in molecular dynamics.

Acknowledgements We wish to thank Prof. Shunji Kishimoto (High-Energy Accelerator Research Organization) for developing the APD detectors. We are also grateful for Mr. Fumitaka Sakai (CFlat Co., Ltd.) for his supplement of images of molecular arrangements of *Ch* phase, *ChBP*_{II} and *Iso* phase (used for Fig. 2). The small-angle X-ray diffraction experiment using Nanopix was performed with a support of Dr. Rintaro Inoue (Kyoto University). The experiment was performed with the approval of the Japan Synchrotron Radiation Research Institute (proposal No. 2017A1096). This work was supported by a Japan Society for the Promotion of Science (JSPS) KAKENHI Grant-in-Aid for Scientific Research (S) (Grant No. JP24221005) and Grant-in-Aid for Young Scientists (B) (Grant No. JP15K17736) and by JST CREST (Grant No. JPMJCR1424), Japan. This work was also partially supported by project for construction of the basis for the advanced materials science

and analytical study by the innovative use of quantum beam and nuclear sciences in Institute for Integrated Radiation and Nuclear Science, Kyoto University.

References

1. Hamley, I.W.: *Introduction to Soft Matter: Polymers, Colloids, Amphiphiles and Liquid Crystals*. Wiley, West Sussex (2000)
2. Kumer, S.: *Liquid Crystals*. Cambridge U. Press, Cambridge (2001)
3. Taheri, B., Muñoz, A.F., Palffy-Muhoray, P., Twieg, R.: Low threshold lasing in cholesteric liquid crystals. *Mol. Cryst. Liq. Cryst.* **358**, 73 (2001)
4. Finkelmann, H., Kim, S.T., Muñoz, A., Palffy-Muhoray, P., Taheri, B.: Tunable mirrorless lasing in cholesteric liquid crystalline elastomers. *Adv. Mater.* **13**, 1069 (2001)
5. Reinitzer, F.: Beiträge zur kenntniss des cholesterins. *Monatsh. Chem.* **9**, 421 (1888)
6. Onusseit, H., Stegemeyer, H.: Observation of direct phase transition smectic A \leftrightarrow blue phase in a liquid crystalline mixed system. *Z. Naturforsch.* **39A**, 658 (1984)
7. de Gennes, P.G., Prost, J.: *The Physics of Liquid Crystals*, 2nd edn. Clarendon, Oxford (1993)
8. Crooker, P.P.: In: Kitzerow, H.S., Bahr, C. (eds.) *Chirality in Liquid Crystals*, p. 186. Springer, New York (2001)
9. Stegemeyer, H., Blumel, T.H., Hiltrop, K., Onusseit, H., Porsch, F.: Thermodynamic, structural and morphological studies on liquid-crystalline blue phases. *Liq. Cryst.* **1**, 3 (1986)
10. Kitzerow, H.S., Crooker, P.P., Heppke, G.: Line shapes of field-induced blue-phase-III selective reflections. *Phys. Rev. Lett.* **67**, 2151 (1991)
11. Hornreich, R.M.: Surface interactions and applied-field effects in cholesteric helicoidal and blue phases. *Phys. Rev. Lett.* **67**, 2155 (1991)
12. Kikuchi, H., Yokota, M., Hisakado, Y., Yang, H., Kajiyama, T.: Polymer-stabilized liquid crystal blue phases. *Nat. Mater.* **1**, 64 (2002)
13. Cao, W., Munoz, A., Palffy-Muhoray, P., Taheri, B.: Lasing in a three-dimensional photonic crystal of the liquid crystal blue phase II. *Nat. Mater.* **1**, 111 (2002)
14. Kitzerow, H.-S., Schmid, H., Heppke, G., Hikmet, R.A.M., Lub, J.: Observation of blue phases in chiral networks. *Liq. Cryst.* **14**, 911 (1993)
15. Baron, A.Q.R., Franz, H., Meyer, A., Rüffer, R., Chumakov, A.I., Burkel, E., Petry, W.: Quasielastic scattering of synchrotron radiation by time domain interferometry. *Phys. Rev. Lett.* **79**, 2823 (1997)
16. Smirnov, G.V., Kohn, V.G., Petry, W.: Dynamics of electron density in a medium revealed by Mössbauer time-domain interferometry. *Phys. Rev. B.* **63**, 144303 (2001)
17. Saito, M., Masuda, R., Yoda, Y., Seto, M.: Synchrotron radiation-based quasi-elastic scattering using time domain interferometry with multiline gamma rays. *Sci. Rep.* **7**, 12558 (2017)
18. Saito, M., Seto, M., Kitao, S., Kobayashi, Y., Kurokuzu, M., Yamamoto, J., Yoda, Y.: Small and large angle quasi-elastic scattering experiments by using nuclear resonant scattering on typical and amphiphilic liquid crystals. *J. Phys. Soc. Jpn.* **81**, 023001 (2012)
19. Saito, M., Yamamoto, J., Masuda, R., Kurokuzu, M., Onodera, Y., Yoda, Y., Seto, M.: Direct observation of interlayer molecular translational motion in a smectic phase and determination of the layer order parameter. *Phys. Rev. Res.* **1**, 012008(R) (2019)
20. Sinha, G., Glorieux, C., Thoen, J.: Broadband dielectric spectroscopy study of molecular dynamics in the glass-forming liquid crystal isopentylcyanobiphenyl dispersed with aerosils. *Phys. Rev. E.* **69**, 031707 (2004)
21. Marik, M., Mukherjee, A., Jana, D., Yoshizawa, A., Chaudhuri, B.K.: Dielectric spectroscopy of T-shaped blue-phase-III liquid crystal. *Phys. Rev. E.* **88**, 012502 (2013)
22. Renn, S.R., Lubensky, T.C.: Abrikosov dislocation lattice in a model of the cholesteric-to-smectic-A transition. *Phys. Rev. A.* **38**, 2132 (1988)
23. Goodby, J.W., Waugh, M.A., Stein, S.M., Chin, E., Pindak, R., Patel, J.S.: Characterization of a new helical smectic liquid crystal. *Nature.* **337**, 449 (1989)
24. Pansu, B., Grelet, E., Li, M.H., Nguyen, H.T.: Hexagonal symmetry for smectic blue phases. *Phys. Rev. E.* **62**, 658 (2000)

Publisher's note Springer Nature remains neutral with regard to jurisdictional claims in published maps and institutional affiliations.

Affiliations

Makina Saito¹ · Jun Yamamoto² · Ryo Masuda¹ · Masayuki Kurokuzu¹ · Yoshitaka Yoda³ · Makoto Seto¹

✉ Makina Saito
msaito@rri.kyoto-u.ac.jp

¹ Institute for Integrated Radiation and Nuclear Science, Kyoto University, Osaka 590-0494, Japan

² Department of Physics Graduate School of Science, Kyoto University, Kyoto 606-8224, Japan

³ Japan Synchrotron Radiation Research Institute, Sayo, Hyogo 679-5198, Japan